Rev.Adv.Mater.Sci. 17(2008) 76-89

NANOGRAIN NUCLEATION THROUGH SPLITTING AND MIGRATION OF GRAIN BOUNDARIES IN DEFORMED NANOMATERIALS

S. V. Bobylev and I. A. Ovid'ko

Institute of Problems of Mechanical Engineering, Russian Academy of Sciences, Bolshoj 61, Vasilievskii Ostrov, St. Petersburg 199178, Russia

Received: January 14, 2008

Abstract. A theoretical model is suggested which describes stress-induced nucleation of nanoscale grains (nanograins) in deformed nanocrystalline metals and ceramics as a process occurring through splitting and migration of grain boundaries. In the framework of the model, nucleation of nanograins is initiated by deformation modes (intergrain sliding, lattice slip, twin deformation, stress-driven migration of grain boundaries) that create disclination dipoles at grain boundaries. The nanograin nucleation occurs through splitting and migration of grain boundaries containing disclination dipoles. It is shown that the nanograin nucleation is energetically favorable in mechanically loaded nanocrystalline Al and α-Al_2O_3 in certain ranges of their parameters and the external stress level.

1. INTRODUCTION

Nanocrystalline materials are fabricated by either "bottom-up" or "top-down" methods [1–3]. The former methods operate with atoms, ions or molecules as starting elements for synthesis of nanoclusters and their aggregates, including bulk and film nanocrystalline materials. The "top-down" methods start with bulk solids having the conventional coarse-grained structure and transform them into nanocrystalline materials (with grain sizes lower than 100 nm). Most "top-down" methods use high-strain plastic deformation processes as those causing grain refinement [1–6]. In doing so, deformation-induced nanocrystallization is commonly treated to occur through continuous dislocation ensemble evolution resulting in consequent formation of dislocation subboundaries, cells and high-angle grain boundaries (GBs) [1–3,6]. Recently, however, computer simulations [7–9] have shown that nanograin nucleation occurs through splitting and migration of GBs near their triple junctions in nanomaterials (with metallic and covalent interatomic bonds) during plastic deformation. The micromechanism and driving forces of the nanograin nucleation reported in Refs. 7–9 are unclear. In Letter [10] we suggested a short theoretical description of the nanograin nucleation in question as a special deformation mode initiated by intergrain sliding and/or lattice slip. In doing so, the nanograin nucleation occurs through splitting and migration of GBs containing disclination dipoles produced by previous plastic deformation. The main aim of this paper is to present in detail and develop the briefly discussed earlier [10] theoretical representations on the nanograin nucleation occurring through splitting and migration of GBs in deformed nanomaterials.

Corresponding author: I.A. Ovid'ko, e-mail: ovidko@def.ipme.ru

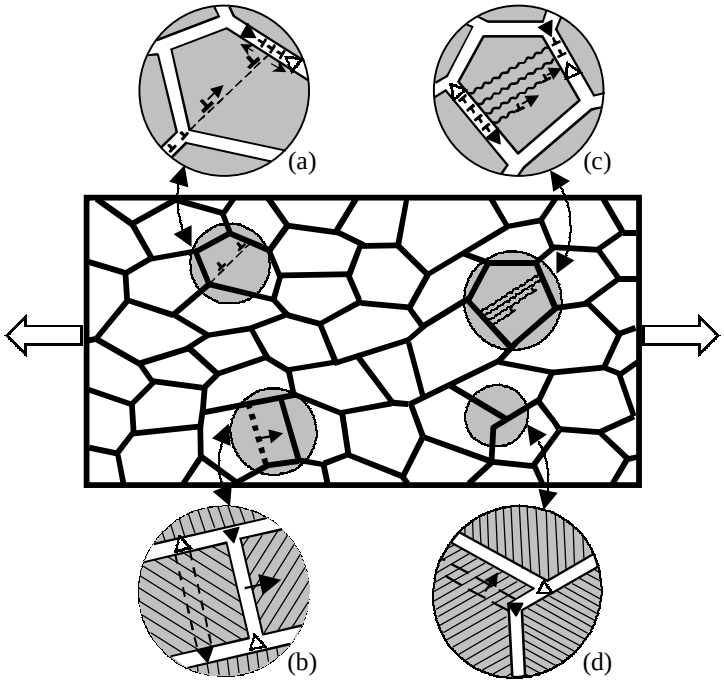

Fig. 1. Transformations of defect structures result in formation of wedge disclination dipoles at grain boundaries and their triple junctions in a deformed nanocrystalline specimen. Magnified insets illustrate formation of disclination dipoles due to (a) slip of lattice dislocations, their absorption at grain boundaries and transformation into wall-like configurations of grain boundary dislocations; (b) stress-driven migration of grain boundaries; (c) twin deformation; and (d) grain boundary sliding and associated movement of triple junctions.

2. DIPOLES OF GRAIN BOUNDARY DISCLINATIONS AS TYPICAL DEFECT STRUCTURES FORMED IN NANOMATERIALS DURING PLASTIC DEFORMATION

Following Letter [10], the nanograin nucleation occurs at dipoles of wedge disclinations at GBs. The wedge disclination dipoles are treated as typical defect structures whose formation in nanomaterials is caused by plastic deformation (Fig. 1). In general, a wedge disclination represents a rotational line defect located at either a GB or a triple junction of GBs and characterized by the disclination strength, the rotational misfit (angle gap) associated with the defect [11,12]. For instance, a wedge disclination at a tilt GB is the line dividing GB fragments with different tilt misorientation angles, whose difference is the disclination strength. A wedge disclination exists at a triple junction of tilt boundaries, if the sum of tilt misorientation angles of these boundaries is non-zero, where summation is performed clockwise along a circuit surrounding the triple junction [11–13]. The strength of the triple junction disclination is the non-zero sum (angle gap) in question.

Let us consider basic micromechanisms responsible for the formation of dipoles of wedge disclinations at GBs in deformed nanomaterials (Figs. 1–5). First, we discuss the disclination dipole formation initiated by the lattice dislocation slip (that often plays the essential role in deformation of nanomaterials [1–3]) (Fig. 2). Lattice dislocations can be produced in nanograins by several ways. For instance, lattice dislocations can be generated by the homogeneous nucleation mechanism [14] and/or they can be emitted from GBs [3] or triple junctions of GBs which carry GB sliding (Fig. 2) [15–17] (as with microcrystalline materials under superplastic deformation [18]). The lattice dislocation slip in a grain interior “supplies” lattice dislocations to a GB [Fig. 2]. The dislocations in the GB are spread into GB dislocations forming a wall-like configuration (Figs. 2c and 2d). As a corollary, tilt

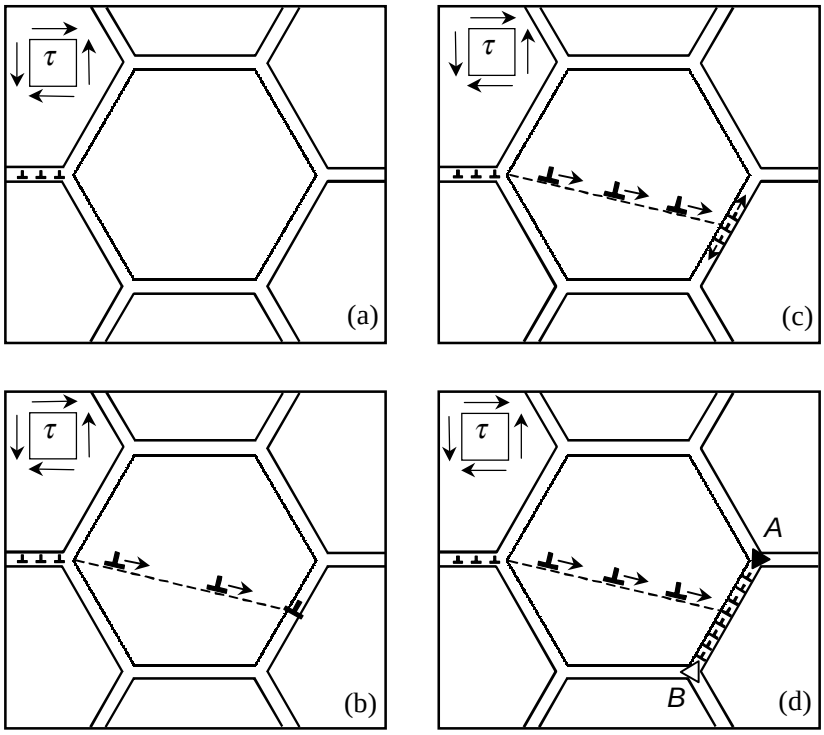

Fig. 2. Formation of a disclination dipole AB at a grain boundary occurs in a deformed nanomaterial due to emission of lattice dislocations from a triple junction of grain boundaries (one of which carries grain boundary sliding); lattice dislocation slip causing "bombardment" of the grain boundary by lattice dislocations; their absorption at the grain boundary and transformation into wall-like configurations of grain boundary dislocations.

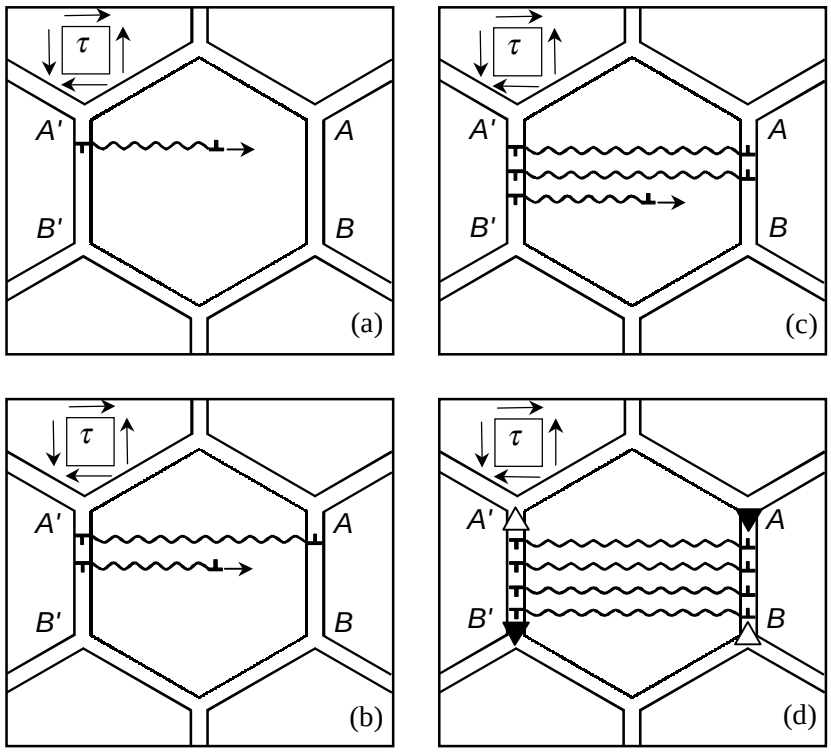

Fig. 3. Formation of a disclination dipole AB at a grain boundary occurs in a deformed nanomaterial due to twin deformation occurring through emission of partial dislocations from grain boundary A'B', their slip in a grain interior, their absorption at grain boundary AB and transformation into wall-like configurations of grain boundary dislocations. A similar disclination dipole is formed at grain boundary A'B'.

misorientation of the GB, after absorption of several dislocations with the same Burgers vectors, changes, say, by value of ω_0, and triple junctions adjacent to the GB become uncompensated (Fig. 2d). In this case, the sums of tilt misorientation angles at the junctions A and B become equal to ω_0 and $-\omega_0$, respectively. In the theory of defects in solids, these junctions are wedge disclinations characterized by the disclination strength $\pm\omega_0$ [11,12]. The disclinations form a dipole configuration (Fig. 2d).

Another way to form GB disclination dipole is related to twin deformation (capable of essentially contributing to plastic flow of nanomaterials [19–24]). This micromechanism is illustrated by Fig. 3 showing the formation of a disclination dipole at a GB AB in a deformed nanomaterial due to twin deformation. The latter occurs through emission of partial dislocations from GB A'B', their slip in a grain interior, their absorption at GB AB and transformation into wall-like configurations of GB dislocations. The wall-like configuration of GB dislocations is equivalent to a dipole of wedge disclinations at junctions A and B (Fig. 3d).

In addition, formation of GB disclination dipoles can be initiated by stress-driven GB migration (capable of essentially contributing to plastic flow of nanomaterials at certain conditions [25–32]). For instance, as shown in Fig. 4, a disclination dipole AB at a GB is generated in a deformed nanomaterial due to stress-driven migration of a GB from its initial position A'B' to the final position AB where the migrating boundary converge with another (immobile) GB; for details, see [27].

Also, GB disclination dipoles typically form in nanomaterials and polycrystals due to interfacial sliding (that dominates, in particular, in superplastic deformation [2,33,34]). Following Ref. 35, interfacial sliding across a triple junction of GBs produces a disclination dipole at a GB fragment along which the triple junction shifts (Figs. 5a and 5b). In short, intergrain sliding along the horizontal GB results in the displacement of both the triple junction (from the position A to the position B) and the vertical GB assumed to be a symmetric tilt boundary with tilt misorientation ω_0. When the triple junction is shifted by intergrain sliding from its initial position A to the position B (Fig. 5b), the angle gaps ω_0 and $-\omega_0$ appear at triple junction (point) A and double junction (point) B at the horizontal GB, respectively [35]. The points A and B are considered as wedge disclinations with the strengths $\pm\omega_0$ [35]. They form a dipole (Fig. 5b).

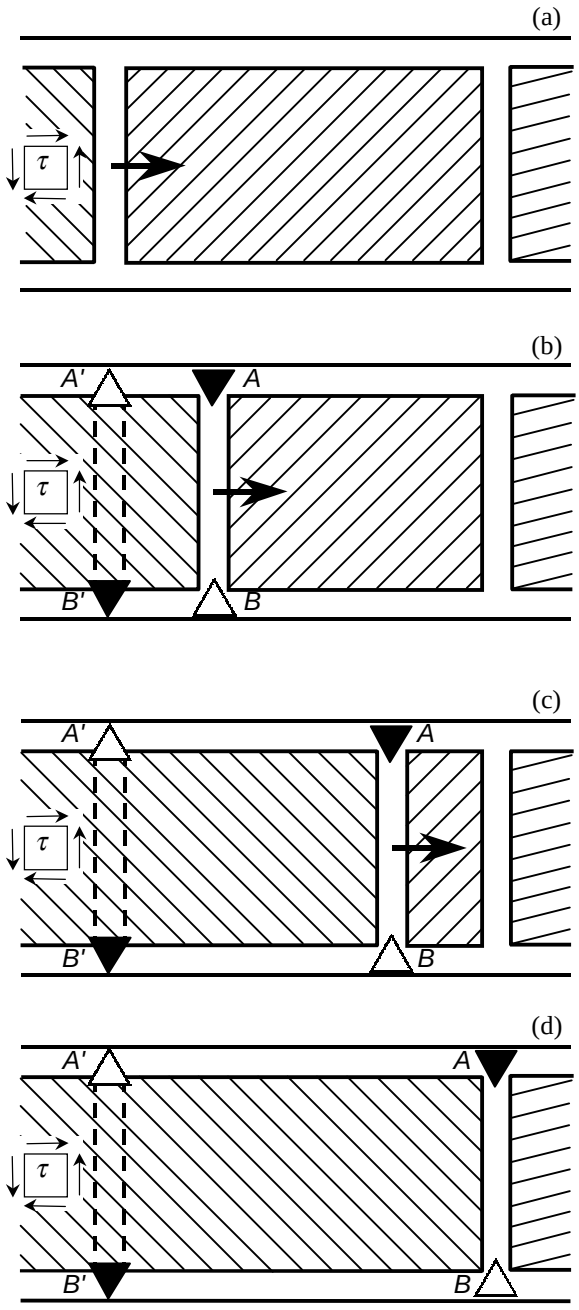

Fig. 4. Formation of a disclination dipole AB at a grain boundary occurs in a deformed nanomaterial due to stress-driven migration of a grain boundary from its initial position A'B' to the final position AB where the migrating boundary converges with another (immobile) grain boundary. Similar disclinations (composing a dipole configuration) are formed at double junctions A' and B' of grain boundaries.

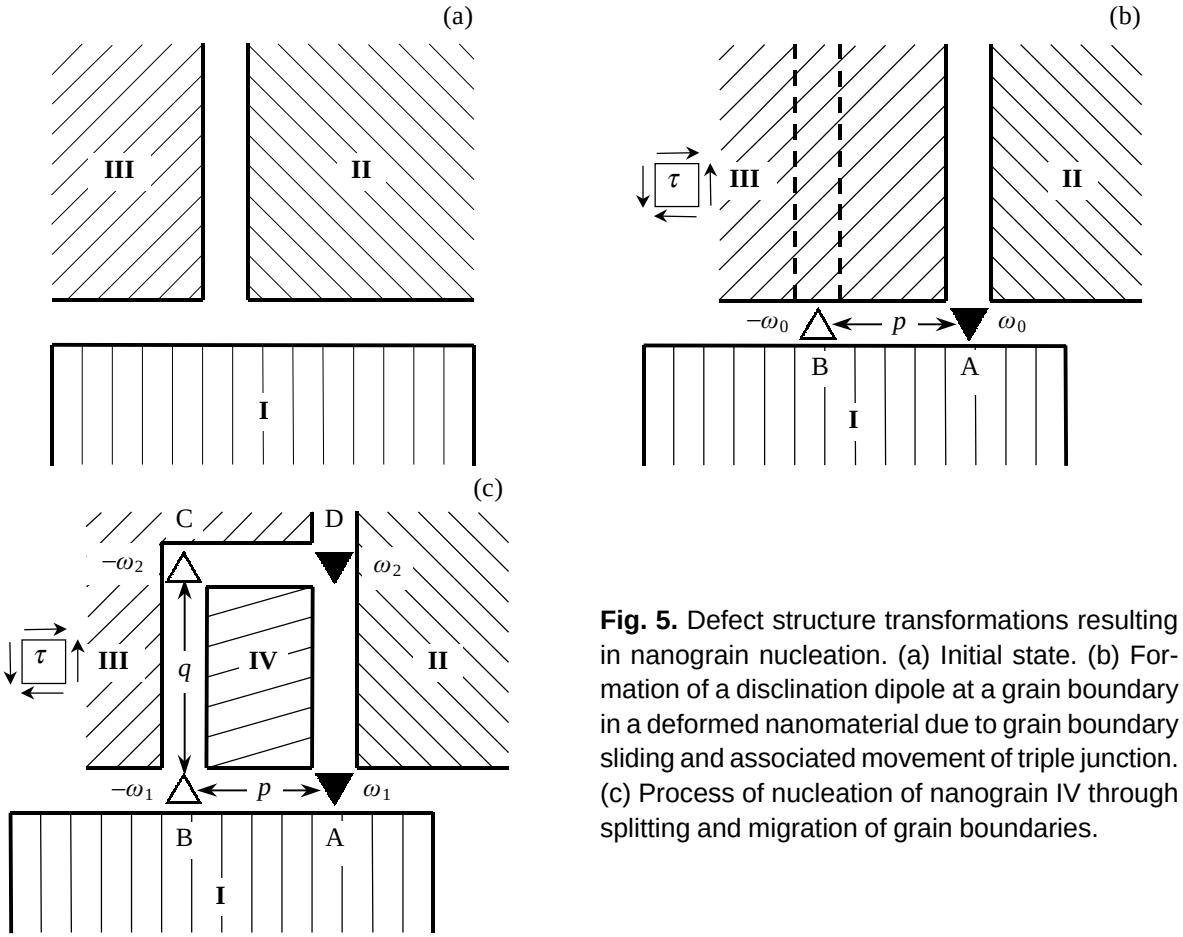

Fig. 5. Defect structure transformations resulting in nanograin nucleation. (a) Initial state. (b) Formation of a disclination dipole at a grain boundary in a deformed nanomaterial due to grain boundary sliding and associated movement of triple junction. (c) Process of nucleation of nanograin IV through splitting and migration of grain boundaries.

3. GEOMETRIC FEATURES OF NANOGRAIN NUCLEATION OCCURRING THROUGH SPLITTING AND MIGRATION OF GRAIN BOUNDARIES IN DEFORMED NANOMATERIALS

GB disclination dipoles under applied stress tend to move causing rotational deformation [11,36]. Also, GB disclinations tend to split, because the splitting is driven by decrease of their elastic energy [11,37]. Combining these processes, one finds that GB disclinations can move and split causing nucleation of a nanograin (nanograin IV), as shown in Fig. 5c. For definiteness, we consider evolution of the disclination dipole shown in Figs. 5b and 5c. The distance between the disclinations of the initial dipole (Fig. 5b) is p. Within our model, the nanograin IV nucleates through splitting of the GB AB into the immobile GB AB and the mobile GB CD (Figs. 5b and 5c). In general, the splitting of the GB is accompanied by the splitting of the initial dipole of GB disclinations with strengths ω_0 and $-\omega_0$ (located at points A and B, respectively; see Fig. 5b) into two dipoles: the immobile dipole of GB disclinations with strengths ω_1 and $-\omega_1$ (located at points A and B, respectively) and the mobile dipole of GB disclinations with strengths ω_2 and $-\omega_2$ (located at points D and C, respectively); see Fig. 5c. For definiteness, we choose misorientations of GBs generated due to the nanograin nucleation (Fig. 5c) as those providing the disclination strength conservation law during the splitting: $\omega_0 = \omega_1 + \omega_2$. The disclination dipole CD moves over distance q in grain III. The crystal lattice in area ABCD swept by the moving GB CD is misoriented relative to lattices in grains I, II and III (Fig. 5c). In this case, the area ABCD represents the nanograin IV whose formation is associated with movement of disclination dipole CD that carries plastic deforma-

tion. As a corollary, the nanograin formation (Fig. 5c) serves as a special deformation mode in nanomaterials and polycrystals.

4. ENERGY CHARACTERISTICS OF NANOGRAIN NUCLEATION OCCURRING THROUGH SPLITTING AND MIGRATION OF GRAIN BOUNDARIES IN DEFORMED NANOMATERIALS

Let us calculate the energy change ΔW (per unit length of a line perpendicular to Fig. 5c) that characterizes the nanograin formation (Fig. 5c). The change ΔW contains the six terms:

$$\Delta W = W_{el}^{\omega_1} + W_{el}^{\omega_2} - W_{el}^{\omega_0} + W_{int} - A + \Delta W_{gb}, \quad (1)$$

Here $_{el}^{\omega_0}$, $_{el}^{\omega_1}$ and $_{el}^{\omega_2}$ are the proper elastic energies of dipole of wedge disclinations with strengths $\pm\omega_0$, $\pm\omega_1$, $\pm\omega_2$, respectively, W_{int} is the energy that characterizes the interaction between the disclination dipoles with strengths $\pm\omega_1$ and $\pm\omega_2$, A is the work spent by the external shear stress τ to movement of the ω_2-dipole, and ΔW_{gb} is the change in the GB energy due to GB splitting that accompanies nucleation of the grain IV.

The proper energies of the disclination dipoles are given by the standard formula [11] as follows:

$$_{el}^{\omega_1} = \frac{D\omega_i^2 p^2}{2}\left(\ln\frac{R}{p} + \frac{1}{2}\right), \; i = 0,1,2, \quad (2)$$

where $D = G/[2\pi(1-\nu)]$, G is the shear modulus, ν is the Poisson ratio, and R is the screening length for stress fields of the disclination dipoles. The energy W_{int} that characterizes the interaction between the disclination dipoles is calculated in the standard way as the work spent to the generation of one disclination dipole in the stress field of another disclination dipole [11,38]. In doing so, one finds:

$$_{int} = D\omega_1\omega_2\left(\frac{p^2+q^2}{2}\ln\frac{R^2}{p^2+q^2} - q^2\ln\frac{R}{q} + \frac{p^2}{2}\right) \quad (3)$$

The work A of the external shear stress τ, spent to movement of the ω_2-dipole is given as [11,38]:

$$A = \tau\omega_2 pq. \quad (4)$$

With formulas (2)–(4) substituted to formula (1), we have:

$$\Delta W = \frac{D\omega_1\omega_2}{2}\left(p^2\ln\frac{p^2}{p^2+q^2} + q^2\ln\frac{q^2}{p^2+q^2}\right) - \tau\omega_2 pq + \Delta W_{gb}. \quad (5)$$

The energy change ΔW_{gb} (per unit length of a line perpendicular to Fig. 5c) due to GB splitting that accompanies nucleation of the grain IV is estimated as $\Delta W_{gb} = \gamma_{gb}(p+q)$, where γ_{gb} is the specific energy of a tilt GB per unit of its area. High-angle GBs can be divided into the two classes: general and special GBs with large and small values of γ_{gb}, respectively [39]. In most materials the GB energy γ_{gb} versus tilt misorientation θ, is a slowly increasing or approximately constant function of θ, for general GBs having tilt misorientation $\theta > 15^o$, with energy "cusps" associated with special GBs in some narrow intervals of θ [39] For simplicity of our consideration focused mostly on high-angle GBs with $\theta > 15^o$, hereinafter, we assume that $\gamma_{gb}(\theta)$ is the constant γ_0, for angles θ of all general GBs, and has the value of $\gamma_1 < \gamma_0$, for angles θ of special GBs. In these circumstances, in accordance with data [39], γ_1 is by several times smaller than γ_0.

With the dramatic difference in the GB energy between general and special GBs, one can distinguish the two following versions of the nanograin nucleation: (1) all GBs involved in the nanograin nucleation process are general; (2) the nanograin nucleation involves one or several special GBs. (We will not consider the situation where one or both of the initial GBs AB and AD (Fig. 5c) are special, because the special GBs during the nanograin nucleation change their misorientation parameters and thereby commonly transform into general GBs. In this situation, the GB energy term ΔW_{gb} essentially increases due to the nanograin nucleation. As a corollary, the situation in question is hardly realized.) In the former case, with our assumption on the dependence $\gamma_{gb}(\theta)$ taken into account, the sum energy of the intial GBs AB and AD does not change, and of the two new GBs BC and CD of lengths q and p, respectively, are formed. In these circumstances, since the energy density of the two new GBs BC and CD is taken as γ_0, the GB energy change ΔW_{gb} is estimated as follows:

$$\Delta W_{gb} = \gamma_0(p+q). \quad (6)$$

Now let us consider the second case where the nanograin nucleation involves one or several special GBs. In this case, ΔW_{gb} depends on sizes of special and general GBs that bound the grain IV. Yamakov *et al.* [7] reported on results of molecular

dynamics simulations of plastic deformation in nanocrystalline Al. The simulations have shown deformation-induced nucleation of a nanograin with two general and two special (more precisely, twin) GBs [7]. In geometry shown in Fig. 5c, the special GBs of the new nanograin are GBs AB and BC. In this context, for the sake of simplicity and definiteness, hereinafter we will consider the only the nucleation of a nanograin with with two general and two special GBs AB and BC (Fig. 5c) (in parallel with the nucleation with all general GBs). In doing so, the GB energy change ΔW_{gb} is represented as:

$$\Delta W_{gb} = \gamma_1 (p + q). \quad (7)$$

Thus, we can find the total energy change ΔW characterizing the nanograin nucleation with the aid of formula (5) and either formula (6) or (7), depending on a nucleation variant.

It is evident that nucleation of a nanograin with two general and two special GBs AB and BC is more energetically favorable than nucleation of a nanograin with all general GBs. However, the generation of a nanograin with two general and two special GBs imposes certain conditions (restrictions) upon both misorientations of GBs and strength of disclinations involved in the nanograin nucleation and strength of disclinations. These restrictions are caused by Kirchhoff rule [12] for GB junctions. The latter, in particular, means that the sum of tilt misorientation angles of GBs joining at a GB junction is equal to the strength of a wedge disclination located at the junction, where summation is performed clockwise along a circuit surrounding the GB junction [11–13]. A detailed consideration of the restrictions caused by Kirchhoff rule [12] for GB junctions is beyond the scope of this paper. Here we just exploit the fact of their existence.

Thus, though the nucleation of a nanograin with both general and special GBs is energetically favorable in most cases (compared to that of a nanograin with general GBs), the nucleation process imposes restrictions on tilt misorientation angles of GBs and strengths of disclinations involved in the process. On the other hand, the nucleation of a nanograin with all general GBs is more conventional process, because it may occur at any set of geometric parameters of the system under consideration. At the same time, its characteristic energy is larger than that in the case of the nucleation of a nanograin with both general and special GBs. In the circumstances discussed, there is interest in calculation of the critical stresses for both nucleation versions.

5. MODEL CALCULATIONS OF CHARACTERISTICS OF NANOGRAIN NUCLEATION IN DEFORMED NANOMATERIALS

With formula (5), we calculated the total energy change ΔW in nanocrystalline Al and nanoceramic α-Al_2O_3. In the calculations, we used the following typical values of parameters: for Al [40], G = 26.5 GPa and ν = 0.34; and, for α-Al_2O_3 [41], G = 169 GPa and ν = 0.23 The grain size (playing role of the upper limit of q and p is taken as d = 15 nm. Following experimental data [42,43], the specific energy of general [110] tilt boundaries with $\theta > 15^o$ in Al is almost insensitive to θ and has value $\gamma_0 \approx 0.4$ J/m^2. At the same time, the dependence $\gamma_{gb}(\theta)$ has two cusps corresponding to twin boundaries with tilt misorientations 70.5° and 129.5°, whose energies are equal to 0.1 and 0.2 J/m^2, respectively. In our further analysis, for definiteness, we consider the only twin boundaries with tilt misorientation 70.5° and energy density assumed to be γ_1 = 0.1 J/m^2 in Al.

In the experiment [44], energies of high-angle tilt boundaries with $\theta > 15^o$ in a α-Al_2O_3 bi-crystal with the [0001] rotation axis were measured. The energies of general GBs were found to be in the range from 0.4 to 0.7 J/m^2. With these data, for definiteness, in our calculations of ΔW in α-Al_2O_3, we use value of γ_0 = 0.5 J/m^2. Also, in the experiment [44], two special GBs (including the twin boundary characterized by misorientation 60°) with energies being around γ_1 = 0.05 J/m^2 in α-Al_2O_3 were identified.

We have calculated typical dependences $\Delta W(q)$ for Al and α-Al_2O_3 (see Figs. 6 and 7, respectively) in the case of $\omega_1 = \omega_2 = 0.5\omega_0$. In this case, the initial disclination dipole splits into the two dipoles characterized by identical disclination strengths. Figs 6a–6c and 7a–7c correspond to the nucleation of nanograins with all general GBs, and the energy ΔW_{gb} is given by formula (6). Figs. 6d–6f and 7d–7f correspond to the nucleation of nanograins with both general and special GBs, and the energy ΔW_{gb} is given by formula (7). Figs. 6 and 7 show evident tendencies that the nanograin nucleation enhances when parameters t, p, ω_0 grow. Also, these figures illustrate the statement that the nucleation of nanograins with both general and special GBs is more energetically favorable than that of nanograins with all general GBs.

Note that the atomistic details of the GB splitting dominate at its very initial stage, for q < 2 nm. To describe such details, atomistic simulations are

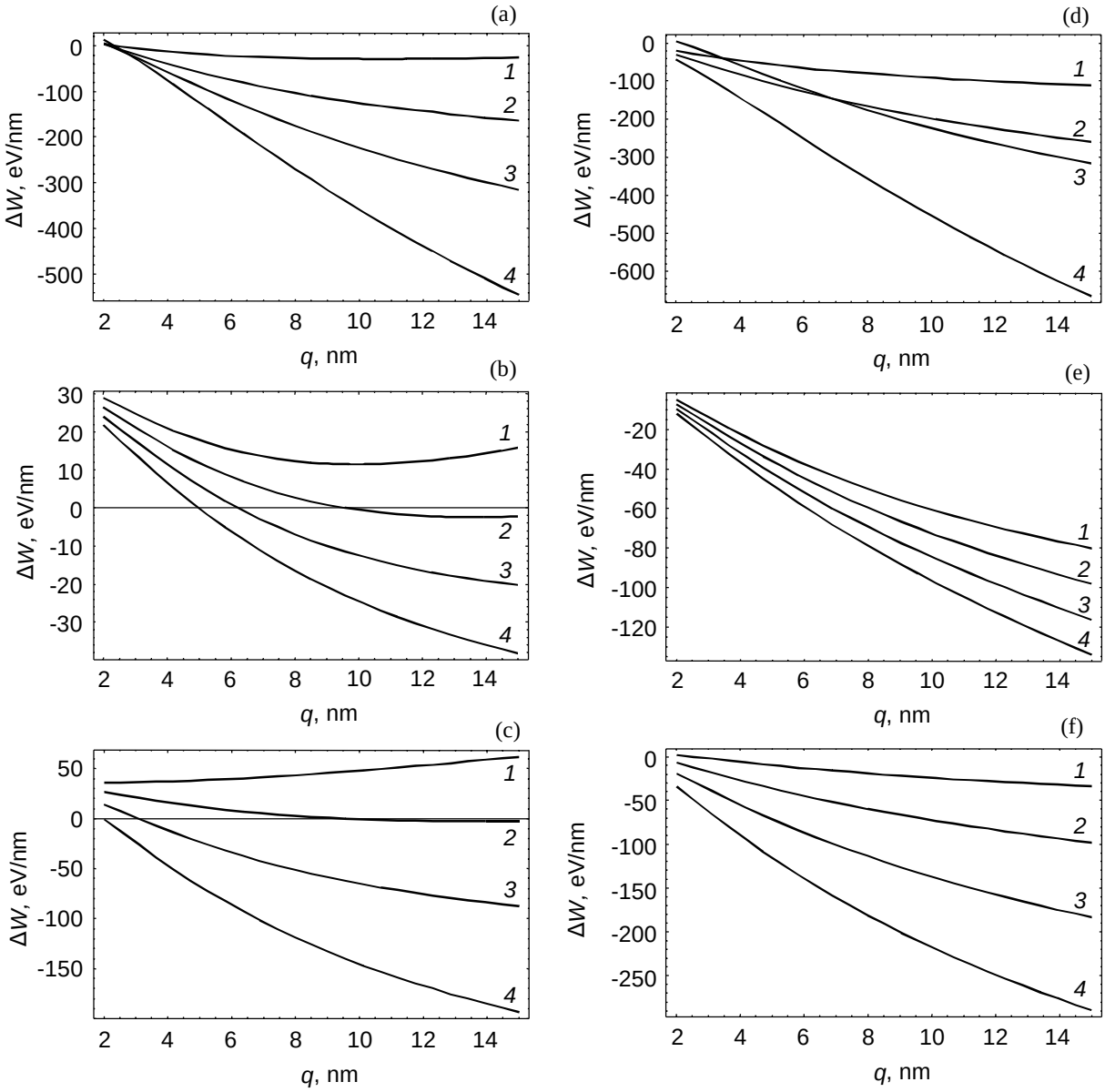

Fig. 6. The dependence of the energy difference ΔW on the distance q moved by grain boundary CD in nanocrystalline Al, in the situation with the nucleation of a nanograin with all general GBs at $\omega_1 = \omega_2 = 0.5\omega_0$, for (a) $\tau = 0.1$ GPa, $\omega_0 = 0.5$ (curves *1, 2, 3* and *4* correspond to $p = 3$, 5, 7 and 10 nm, respectively); (b) $p = 5$ nm, $\omega_0 = 0.3$ (curves *1, 2, 3* and *4* correspond to values of $\tau = 0.1$, 0.2, 0.3 and 0.4 GPa, respectively); (c) $p = 5$ nm, $\tau = 0.2$ GPa (curves *1, 2, 3* and *4* correspond to values of $\omega_0 = 0.2$, 0.3, 0.4 and 0.5, respectively); *d*, *e*, *f* the dependences $\Delta W(q)$ are presented for the same values of parameters as with the dependences $\Delta W(q)$ presented in *a*, *b*, *c*, respectively, but in the situation with the nucleation of a nanograin having two general and two special GBs.

needed which are beyond the scope of our continuum approach. At the same time, the energy profit of the GB splitting in the range of $q \geq 2$ nm is critical for the splitting to occur, because the very initial stage ($q < 2$ nm) may occur through thermally-assisted formation of steps at the initial GB, if the splitting of the GB at $q \geq 2$ nm is energetically favorable. In this context, we will focus our analysis to the situation where $p, q \geq 2$ nm. In this situation, the nucleation of the grain IV (Fig. 5c) is char-

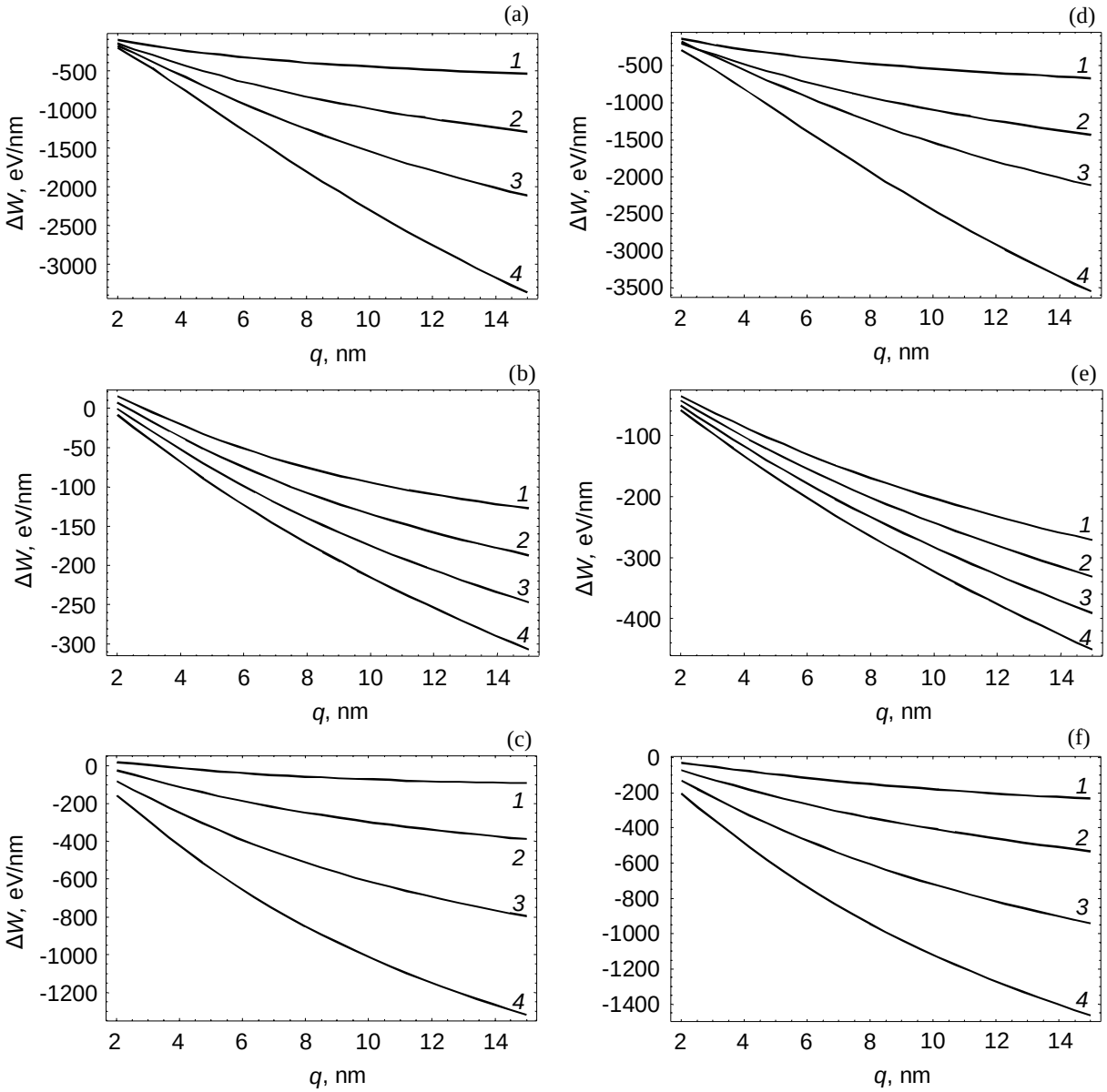

Fig. 7. The dependence of the energy difference ΔW on the distance q moved by grain boundary CD in nanocrystalline α-Al_2O_3, in the situation with the nucleation of a nanograin with all general GBs at $\omega_1 = \omega_2 = 0.5\omega_0$, for (a) $\tau = 0.1$ GPa, $\omega_0 = 0.5$ (curves *1, 2, 3* and *4* correspond to $p = 3$, 5, 7 and 10 nm, respectively); (b) $p = 5$ nm, $\omega_0 = 0.3$ (curves *1, 2, 3* and *4* correspond to values of $\tau = 0.5$, 1.0, 1.5 and 2.0 GPa, respectively); (c) $p = 5$ nm, $\tau = 0.2$ GPa (curves *1, 2, 3* and *4* correspond to values of $\omega_0 = 0.2$, 0.3, 0.4 and 0.5, respectively); *d*, *e*, *f* the dependences $\Delta W(q)$ are presented for the same values of parameters as with the dependences $\Delta W(q)$ presented in *a*, *b*, *c*, respectively, but in the situation with the nucleation of a nanograin having two general and two special GBs.

acterized by the absence of any energy barrier, if the following inequalities are valid:

$$\Delta W\left(q = 2\,\text{nm}\right) \le 0, \tag{8}$$

$$\left.\frac{\partial\left(\Delta W\right)}{\partial q}\right|_{q=2\,\text{nm}} \le 0. \tag{9}$$

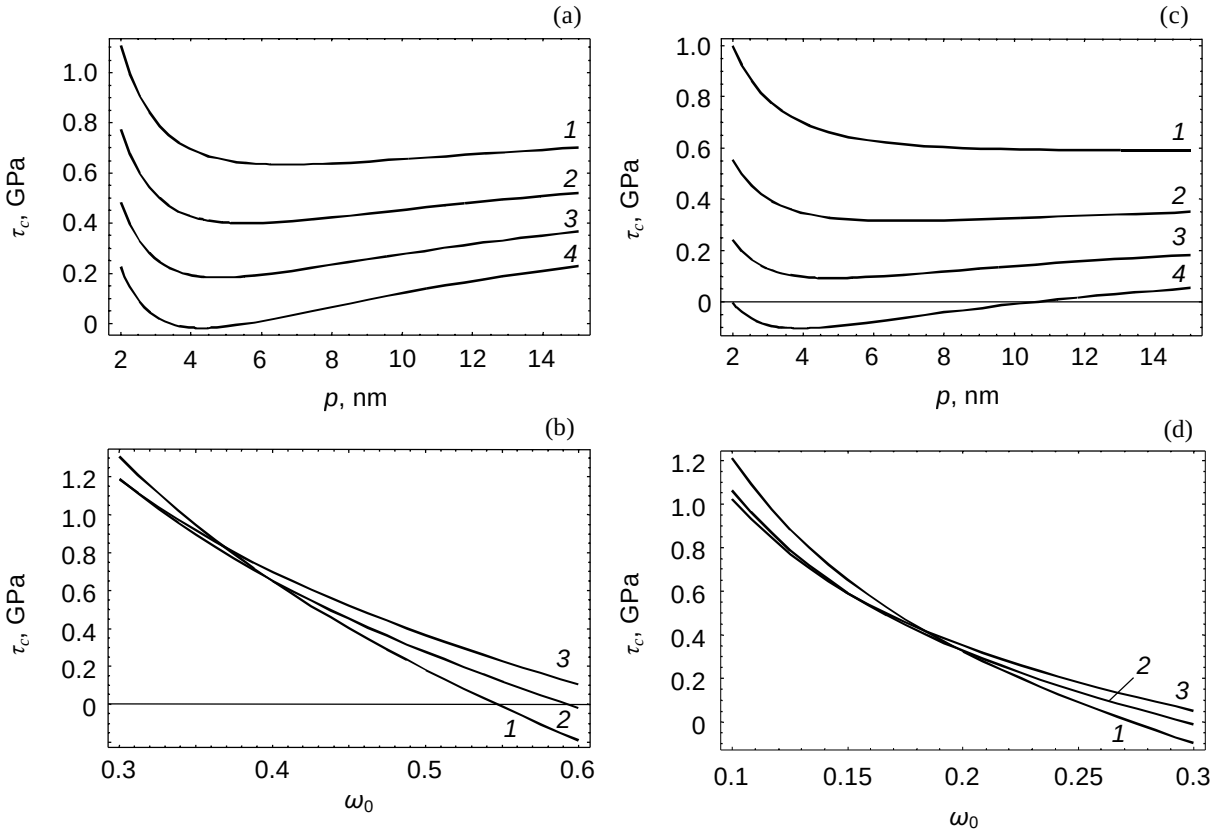

Fig. 8. The dependence of the critical shear stress τ_c in nanocrystalline Al (a) on the size p of the disclination dipole AB in the situation with the nucleation of a nanograin with all general GBs (curves *1, 2, 3* and *4* correspond to ω_0 = 0.4, 0.45, 0.5 and 0.55, respectively); (b) on parameter ω_0 in the situation with the nucleation of a nanograin with all general GBs (curves *1, 2* and *3* correspond to p = 5 10 and 15 nm, respectively); (c) on the size p of the disclination dipole AB in the situation with the nucleation of a nanograin having two general and two special GBs (curves *1, 2, 3* and *4* correspond to ω_0 = 0.15, 0.2, 0.25 and 0.3, respectively); (d) on parameter ω_0 in the situation with the nucleation of a nanograin having two general and two special GBs (curves *1, 2* and *3* correspond to p = 5, 10 and 15 nm, respectively).

In terms of the applied stresses, the non-barrier nucleation of the grain IV (Fig. 5c) occurs, if the applied shear stress reaches its critical value τ_c. The latter is defined as the minimum stress at which both inequalities (8) and (9) are valid. With formulas (5), (6), (8), and (9), after some algebra, we find the following expression for τ_c characterizing the non-barrier nucleation of the grain with all general GBs in realistic ranges of parameters of nanocrystalline Al and Al_2O_3:

$$\tau_c = \left[\frac{D\omega_1}{2} \left(\frac{p}{q} \ln \frac{p^2}{p^2+q^2} + \frac{q}{p} \ln \frac{q^2}{p^2+q^2} \right) + \frac{\gamma_0 (p+q)}{\omega_2 pq} \right]_{q=2\,\mathrm{nm}} . \quad (10)$$

In the case of the nucleation of nanograins with both general and special GBs, γ_0 should be replaced by γ_1 in formula (10).

Figs. 8 and 9 present the dependence of τ_c on p, calculated by formula (6), in the cases of Al and α-Al_2O_3, respectively. Figs. 8a, 8b and 9a, 9b correspond to the nucleation of nanograins with all general GBs. Figs. 8c, 8d and 9c, 9d correspond to the nucleation of nanograins with both general and special GBs. In doing so, we considered the splitting characterized by the relationship: $\omega_1 = \omega_2 = 0.5\omega_0$. Curves presented in Figs. 8 and 9 show that the critical shear stress τ_c weakly depends on parameter p and, on the contrary, is highly sensitive to the disclination strength ω_0 characterizing the initial disclination dipole. Also, as it follows from Fig.

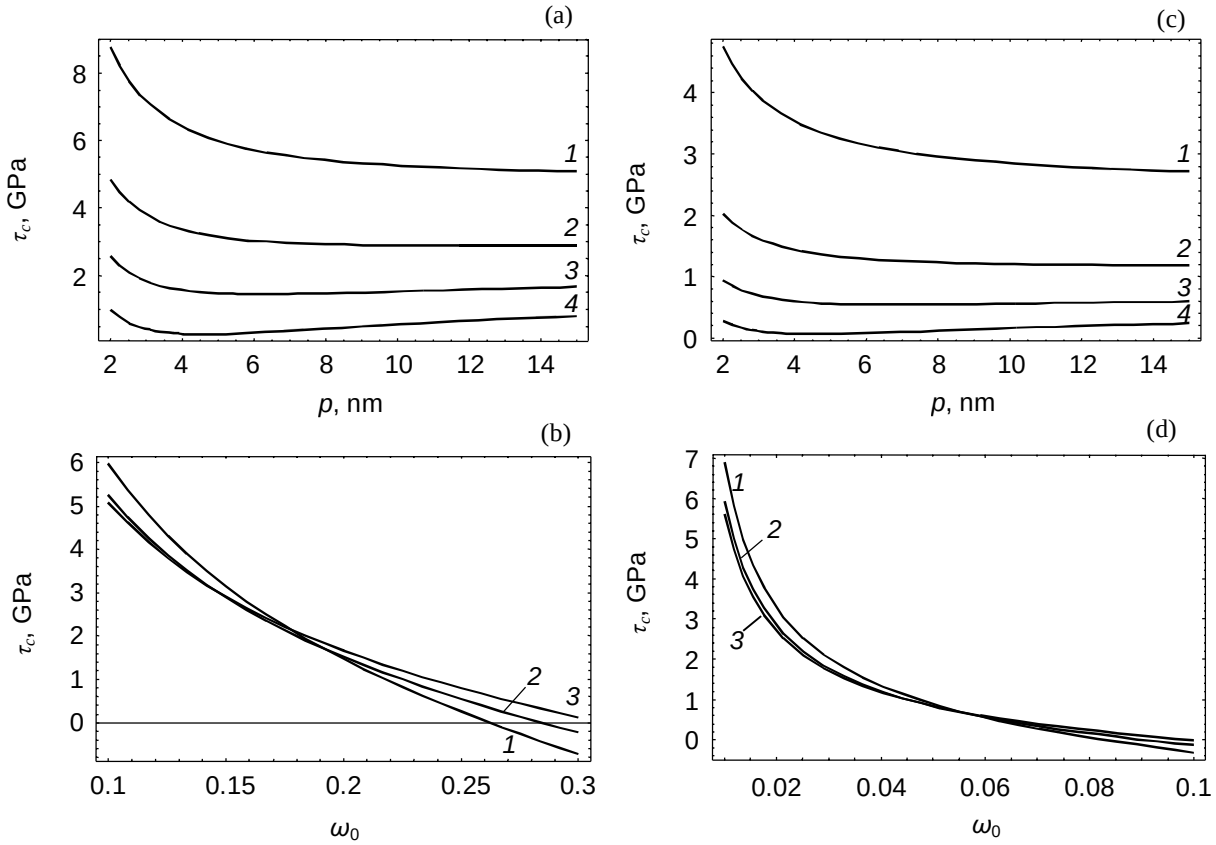

Fig. 9. The dependence of the critical shear stress τ_c in nanocrystalline α-Al_2O_3 (a) on the size p of the disclination dipole AB in the situation with the nucleation of a nanograin with all general GBs (curves *1, 2, 3* and *4* correspond to ω_0 = 0.1, 0.15, 0.2 and 0.25, respectively); (b) on parameter ω_0 in the situation with the nucleation of a nanograin with all general GBs (curves *1, 2* and *3* correspond to p = 5, 10 and 15 nm, respectively); (c) on the size p of the disclination dipole AB in the situation with the nucleation of a nanograin having two general and two special GBs (curves *1, 2, 3* and *4* correspond to ω_0 = 0.02, 0.04, 0.06 and 0.08, respectively); (d) on parameter ω_0 in the situation with the nucleation of a nanograin having two general and two special GBs (curves *1, 2* and *3* correspond to p = 5, 10 and 15 nm, respectively).

8b, for $\omega_0 > 0.5$, the critical shear stress τ_c for the nucleation of a nanograin with all general GBs is lower than $\tau \approx 0.3$ GPa, which is realistic for nanocrystalline Al. Also, as it follows from Fig. 9b, for $\omega_0 > 0.15$, the critical shear stress τ_c for the nucleation of a nanograin with all general GBs is lower than $\tau \approx 3.5$ GPa, which is realistic for nanocrystalline α-Al_2O_3. In the case of the nucleation of a nanograin with both general and special GBs, values of ω_0, at which the critical stress τ_c achieves values that can be reached in real materials are lower than those in the case of the nucleation of a nanograin with all general GBs. In particular, realistic values of the critical stress τ_c correspond to $\omega_0 > 0.2$ in Al (Fig. 8d) and $\omega_0 > 0.02$ in α-Al_2O_3 (Fig. 9d).

Note that curves in Figs. 8c, 8d and 9c, 9d, corresponding to the nucleation of nanograins with both general and special GBs, formally are presented in the interval of values of ω_0. Nevertheless, as it was noted in section 4, the nucleation of nanograins with both general and special GBs imposes restrictions on the tilt misorientation of GBs and strengths of disclinations. Since ω_0 directly depends on tilt misorientations of GBs involved in the grain nucleation process, ω_0 should have a certain value (with the proviso that $\omega_1 = \omega_2 = 0.5\omega_0$). However, in general, the relationship between

disclination strengths and GB misorientations is ambiguous and depends on mechanism of the nanograin nucleation, in parallel with other factors. In these circumstances, the relationship in question can not be formulated in the universal form. Each concrete situation should be analysed in a separate way. With this taken into account, curves presented in Figs. 8 and 9 are rather informative and useful, because they can be exploited in any situation. Their adoption to a concrete situation can be done by an appropriate choice of ω_0 corresponding to the concrete defect configuration under consideration.

It should be noted that, when ω_0 increases, the critical stress τ_c can decrease up to negative values. This aspect follows from formula (10) having the first term on its right-hand side, which is always negative and decreases with rizing ω_0 (with the proviso that $\omega_1 = 0.5\omega_0$). This behavior is caused by the fact that a profit in the energy of the defect system grows parallel with ω_0^2 due to the splitting of the ω_0-disclination dipole. Negative values of τ_c mean that the splitting of the ω_0-disclination dipole occurs, even if the external stress hampers the splitting process.

In our calculations we used the splitting version characterized by relation $\omega_1 = \omega_2 = 0.5\omega_0$, which yields the largest decrease in the elastic energy of the disclination system in the absence of the external stress τ. When τ acts in a nanocrystalline specimen, the most energetically favorable splitting version is characterized by inequality $\omega_2 > \omega_1$. This fact is illustrated in Fig. 10 showing the dependences of parameter ω_2/ω_0, corresponding to the most energetically favorable splitting version, on the external stress τ. The energy profit was determined by position of the initial point of the dependence $\Delta W(q)$ at q = 2 nm. The lowest value of ΔW in this point determines the most energetically favorable defect configuration. Data for Al and α-Al_2O_3 are presented in Figs. 10a and 10b, respectively. Curves 1, 2, 3, 4 and 5 are calculated for p = 5 nm and correspond to values of ω_0 = 0.1, 0.2, 0.3, 0.4 and 0.5, respectively. It is evident that, when t grows, the configurations with growing ω_2 become more energetically favorable. At some value of τ, the limiting situation with $\omega_1 = 0$, $\omega_2 = \omega_0$ (see curve 1 in Fig. 10) comes into play.

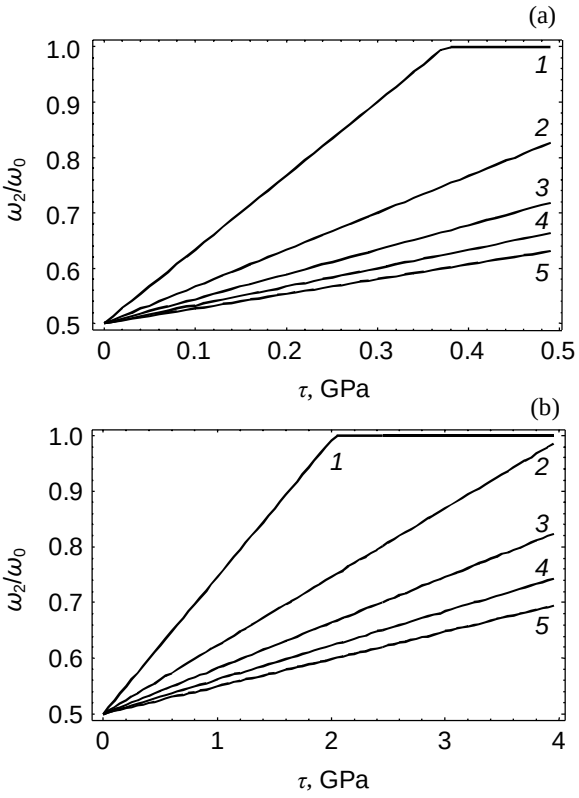

Fig. 10. Dependence of the ratio ω_2/ω_0 (at which the nanograin nucleation is most favourable) on the external stress t. Curves *1, 2, 3, 4* and *5* correspond to values of ω_0 = 0.1, 0.2, 0.3, 0.4 and 0.5, respectively. They are presented in the case of p = 5 nm.

6. DISCUSSION. CONCLUDING REMARKS

In summary, we have theoretically described stress-induced nucleation of nanograins in deformed nanomaterials as a process occurring through splitting and migration of GBs. The nucleation of nanograins is initiated by deformation modes (intergrain sliding, lattice slip, twin deformation, stress-driven migration of grain boundaries) that create disclination dipoles at GBs. The nanograin nucleation occurs through splitting and migration of GBs containing disclination dipoles.

In the framework of the suggested model, it has been shown that the stress-induced nucleation of nanograins occurs in the energy non-barrier way in nanocrystalline Al and α-Al_2O_3 in certain ranges of their parameters and the applied stress level. Our model accounts for results of computer simulations [7–9] and experiments [45,46] showing grain nucleation at triple junctions of GBs in deformed nanomaterials and polycrystals. In particular, we have considered two versions of the nanograin

nucleation: the nucleation process resulting in nanograin with all general GBs and that resulting in nanograin with two general and two special GBs. The latter is more energetically favorable, but imposes certain geometric restrictions on misorientation parameters of GBs and strengths of disclinations involved in the nanograin nucleation process.

In general, nanocrystalline metals and ceramics in the course of plastic deformation often show the outstanding mechanical characteristics attributed to the effects of the nanocrystalline structure; see, e.g., [1-3, 33, 34, 47–55]. On the other hand, the nanocrystalline structure can be formed in initially coarse-grained materials due to deformation processes [1-3]. The deformation-induced nucleation of nanograins in nanocrystalline metals and ceramics, revealed in computer simulations [7–9] and theoretically considered in this paper, represents a new manifestation of close relationship between the nanostructure and the unique mechanical behavior of these materials. More precisely, the nanograin nucleation serves as a special mode of plastic deformation in nanomaterials.

The work was supported, in part, by the Russian Federal Agency of Science and Innovations (Contract 02.513.11.3190 of the Program "Industry of Nanosystems and Materials"), the National Science Foundation (grant CMMI #0700272), Russian Academy of Sciences Program "Structural Mechanics of Materials and Construction Elements", and St. Petersburg Center of the Russian Academy of Sciences.

References

[1] C.C. Koch // *Rev. Adv. Mater. Sci.* **5** (2003) 91.
[2] C. C. Koch // *J. Mater. Sci.* **42** (2007) 1403.
[3] C. C. Koch, I. A. Ovid'ko, S. Seal and S. Veprek, *Structural Nanocrystalline Materials: Fundamentals and Applications* (Cambridge U. Press, Cambridge, 2007).
[4] T.G. Langdon // *Rev. Adv. Mater. Sci.* **13** (2006) 6.
[5] R.Z. Valiev and T.G. Langdon // *Rev. Adv. Mater. Sci.* **13** (2006) 15.
[6] H.J. Fecht, E. Hellstern, Z. Fu and W.L. Johnson // *Met. Trans. A* **21** (1990) 2333.
[7] V. Yamakov, D. Wolf, S.R. Phillpot, A.K. Mukherjee and H. Gleiter // *Nature Mater.* **1** (2002) 45.
[8] M.J. Demkowicz, A.S. Argon, D. Farkas and M. Frary // *Philos. Mag.* **87** (2007) 4253.
[9] A.Cao and Y. Wei // *Phys. Rev. B* **76** (2007) 024113.
[10] S.V. Bobylev and I.A. Ovid'ko // *Appl. Phys. Lett.* **92** (2008) 081914.
[11] A. E. Romanov and V. I. Vladimirov, In: *Dislocations in Solids*, ed. by F. R. N. Nabarro (North Holland, Amsterdam, 1992), Vol. 9, p.191.
[12] M. Kleman and J. Friedel // *Rev. Mod. Phys.* **80** (2008) 61.
[13] G. Dimitrakopulos, Ph. Komminou, Th. Karakostas and R.C. Pond // *Interface Sci.* **7** (1999) 217.
[14] M.Yu. Gutkin and I.A. Ovid'ko // *Appl. Phys. Lett.* **88** (2006) 211901.
[15] A.A.Fedorov, M.Yu. Gutkin and I.A. Ovid'ko // *Acta Mater.* **51** (2003) 887.
[16] F.A. Mohamed and M.Chauhan // *Metall. Mater. Trans. A* **37** (2006) 3555.
[17] F.A. Mohamed // *Metall. Mater. Trans. A* **38** (2007) 340.
[18] O.A. Ruano, J. Wadsworth and O.D. Sherby // *Acta Mater.* **51** (2003) 3617.
[19] M. Chen, E. Ma, K.J. Hemker, H. Sheng, Y. Wang and X. Cheng // *Science* **300** (2003) 1275.
[20] X.Z. Liao, F. Zhou, E.J. Lavernia, S.G. Srinivasan, M.I. Baskes, D.W. He and Y.T. Zhu // *Appl. Phys. Lett.* **83** (2003) 632.
[21] X.Z. Liao, F. Zhou, E.J. Lavernia, D.W. He and Y.T. Zhu // *Appl. Phys. Lett.* **83** (2003) 5062.
[22] X.Z. Liao, Y.H. Zhao, S.G. Srinivasan, Y.T. Zhu, R.Z. Valiev and D.V. Gunderov // *Appl. Phys. Lett.* **84** (2004) 592.
[23] Y.T. Zhu, X.Z. Liao and R.Z. Valiev // *Appl. Phys. Lett.* **86** (2005) 103112.
[24] Y.M Wang, A.M. Hodge, J. Biener, A.V. Hamza, D.E. Barnes, K. Liu and T.G. Nieh // *Appl. Phys. Lett.* **86** (2005) 101915.
[25] M. Jin, A.M. Minor, E.A. Stach and J.W. Morris Jr. // *Acta Mater.* **52** (2004) 5381.
[26] W.A. Soer, J.Th.M. De Hosson, A.M. Minor, J.W. Morris Jr. and E.A. Stach // *Acta Mater.* **52** (2004) 5783.
[27] M.Yu. Gutkin and I.A. Ovid'ko // *Appl. Phys. Lett.* **87** (2005) 251916.
[28] J.Th.M. De Hosson, W.A. Soer, A.M. Minor, Z. Shan, E.A. Stach, S.A. Syed Asif and O.L. Warren // *J. Mater. Sci.* **41** (2006) 7704.
[29] K. Zhang, J.R. Weertman and J.A. Eastman // *Appl. Phys. Lett.* **85** (2004) 5197; **87** (2005) 061921.

[30] P.L. Gai, K. Zhang and J. Weertman // *Scripta Mater.* **56** (2007) 25.
[31] X.Z. Liao, A.R. Kilmametov, R.Z. Valiev, H. Gao, X. Li, A.K. Mukherjee, J.F. Bingert and Y.T. Zhu // *Appl. Phys. Lett.* **88** (2006) 021909.
[32] D. Pan, T.G. Nieh and M.W. Chen // *Appl. Phys. Lett.* **88** (2006) 161922.
[33] D. Wolf, V. Yamakov, S. R. Phillpot, A. K. Mukherjee and H. Gleiter // *Acta Mater.* **53** (2005) 1.
[34] M. Dao, L. Lu, R. J. Asaro, J.Th.M. De Hosson and E. Ma // *Acta Mater.* **55** (2007) 4041.
[35] I.A. Ovid'ko and A.G. Sheinerman // *Appl. Phys. Lett.* **90** (2007) 171927.
[36] I. A. Ovid'ko // *Science* **295** (2002) 2386.
[37] M.Yu. Gutkin and I.A. Ovid'ko, *Plastic Deformation in Nanocrystalline Materials* (Springer, Berlin, 2004).
[38] T. Mura, *Micromechanics in solids* (Martinus Nijhoff, Dordrecht, 1987).
[39] A.P. Sutton and R.W. Balluffi, *Interfaces in Crystalline Materials* (Clarendon, Oxford, 1995).
[40] J. P. Hirth and J. Lothe, *Theory of Dislocations* (Wiley, New York, 1982).
[41] R.G. Munro // *J. Am. Ceram. Soc.* **80** (1997) 1919.
[42] A. Otsuki and M. Mizuno, *Grain Boundary Structure and Related Phenomena*, Suppl. Trans. JIM **27** (Japan Institute of Metals, 1986) p. 789.
[43] G.C. Hasson and C. Goux // *Scripta Metall.* **5** (1971) 889.
[44] T. Watanabe, H. Yoshida, T. Saito, T. Yamamoto, Y. Ikuhara and T. Sakuma // *Mater. Sci. Forum* **304**–**306** (1999) 601.
[45] H. Miura, T. Sakai, H. Hamaji and J.J. Jonas // *Scripta Mater.* **50** (2004) 65.
[46] H. Miura, T. Sakai, S. Andriawanto and J.J. Jonas // *Philos. Mag.* **85** (2005) 2653.
[47] I.A. Ovid'ko, A.G. Sheinerman and N.V. Skiba // *Rev. Adv. Mater. Sci.* **16** (2007) 102.
[48] A. Shukla, V. Parameswaran, Y. Du and V. Évora // *Rev. Adv. Mater. Sci.* **13** (2006) 44.
[49] H. Klostermann, F. Fietzke, T. Modes and O. Zywitzki // *Rev. Adv. Mater. Sci.* **15** (2007) 33.
[50] A.M. Saad, V.A. Kalaev, J.A. Fedotova, K.A. Sitnikov, A.V. Sitnikov, Yu.E. Kalinin, A.K. Fedotov and V.A. Svito // *Rev. Adv. Mater. Sci.* **15** (2007) 208.
[51] A. Akbari, J.P. Riviere, C. Templier, E. Le Bourhis and G. Abadias // *Rev. Adv. Mater. Sci.* **15** (2007) 111.
[52] S.V. Bobylev, N.F. Morozov and I.A. Ovid'ko // *Rev. Adv. Mater. Sci.* **13** (2006) 77.
[53] A.V. Sergueeva and A.K. Mukherjee // *Rev. Adv. Mater. Sci.* **13** (2006) 1.
[54] F. Ebrahimi, A. J. Liscano, D. Kong, Q. Zhai and H. Li // *Rev. Adv. Mater. Sci.* **13** (2006) 33.
[55] I.A. Ovid'ko and A.G. Sheinerman // *Rev. Adv. Mater. Sci.* **16** (2007) 1.